First principles calculation of phonon dispersion, thermodynamic properties and *B* 1-to-*B* 2 phase transition of lighter alkali hydrides

2007 J. Phys.: Condens. Matter 19 086209

(http://iopscience.iop.org/0953-8984/19/8/086209)

IOP PUBLISHING JOURNAL OF PHYSICS: CONDENSED MATTER

J. Phys.: Condens. Matter **19** (2007) 086209 (15pp) doi:10.1088/0953-8984/19/8/086209

First principles calculation of phonon dispersion, thermodynamic properties and $B1$-to-$B2$ phase transition of lighter alkali hydrides

Wen Yu[1,2], **Changqing Jin**[1] **and Axel Kohlmeyer**[3]

[1] Institute of Physics, Chinese Academy of Sciences, PO Box 603, Beijing 100080, People's Republic of China
[2] Physics Department, University of Science and Technology, Beijing, Beijing 100083, People's Republic of China
[3] Department of Chemistry, Center for Molecular Modeling, University of Pennsylvania, 231 South 34th Street, Philadelphia, PA 19104-6323, USA

Received 21 August 2006, in final form 19 December 2006
Published 9 February 2007
Online at stacks.iop.org/JPhysCM/19/086209

Abstract

The phonon dispersions of LiD, LiH and NaH for $B1$ and $B2$ phases are computed using density-functional perturbation theory (DFPT) with both local density (LDA) and generalized gradient (GGA) approximations. It is found from the phonon dispersion curves that the $B2$ phase is unstable at low pressure for all the systems considered. From the vibrational free energy, the coefficient of the linear thermal expansion, the heat capacity and the vibrational entropy as a function of temperature at zero pressure are calculated within the framework of the quasiharmonic approximation. Very good agreement is found for these properties except in the case of the GGA at high temperature. The equation of states for NaH $B1$ and $B2$ phases at 300 K and the $B1$-to-$B2$ phase transition pressure are in excellent agreement with experimental results. The equation of state for the LiH $B1$ phase agrees well with experiments and recent theoretical calculations. The estimated $B1$-to-$B2$ phase transition pressure (308 GPa) is also in good agreement with other theoretical calculations.

1. Introduction

As the lightest alkali hydride, lithium hydride (LiH) exits in the rock-salt structure ($B1$) under normal conditions. Although its electronic, structural and compression properties have been studied extensively [1–8] because of their important usage in thermonuclear and potential energy supplies, there still remain some open issues, among which are the impact of the large zero-point motion, and existence of a rock-salt ($B1$) to caesium chloride ($B2$) phase transition, which has been found in all other alkali hydrides [9]. The first issue been addressed by several authors recently [6, 10–13], and it is found that the zero point motion plays a crucial role in accurately determining the lattice constant and bulk modulus of LiH. The second one is more

subtle, because it intertwines with the metal–insulator transition (MIT) in the $B1$ phase [3, 11]. To make things worse, theoretical calculations [4, 11] predicted the MIT pressures around 200 GPa, which is almost 200 GPa lower than the experimental extrapolation value [8]. This is, however, mainly due to an underestimation of the energy gap of insulators by the DFT method [14]. As a consequence, DFT calculations on LiH using LDA show that MIT should happen first, followed by the $B1$-to-$B2$ transition. Recently, Lebègue *et al* studied this question using the GW method and found a simultaneous structural-phase and metal–insulator transition pressure of 329 GPa [11], which is close to the theoretical $B1$-to-$B2$ transition pressure of 313 GPa given by Wang *et al* [15].

The first issue is mainly addressed within the framework of quasiharmonic approximation (QHA). Under the QHA, the frequencies depend only on volume, not on temperature; i.e., at each volume, the modes behave harmonically and can only change amplitudes without changing frequencies. But it is essential to calculate the full phonon spectrum as a function of volume. Since this is computationally too demanding, only recently have there been some attempts to calculate the temperature dependence of the lattice parameter and bulk modulus.

On the other hand, it has been demonstrated that the Compton profiles of LiH calculated by the pseudopotential method excluding the core electrons of lithium are in rather poor agreement with experiment [16]. The reason for this is the inability for the pseudopotential to generate a realistic valence-charge density in the core region of lithium.

In this paper, we computed the full phonon dispersions of LiH, LiD and NaH for the $B1$ and $B2$ phases within a wide range of volume and calculated the temperature dependence of lattice parameters, bulk modulus and the thermodynamic properties to check the validity of the QHA in the case of large zero-point motion and the effect of core electrons in the case of alkali hydrides. The phonon spectra of LiH and LiD in the $B1$ phase have been calculated by Roma *et al* [10] and Ke *et al* [28] calculated the phonon dispersion curves as well as the entropy as a function of temperature at zero pressure for the NaH $B1$ phase. But to our knowledge, no thermal dynamic properties have been calculated for lithium hydride and its isotopes by the QHA and no phonon dispersion calculation has been performed on the $B2$ phase of alkali hydrides.

2. Theoretical background

2.1. Quasiharmonic approximation and thermodynamic properties

Within the framework of the quasiharmonic approximation, the Helmholtz free energy can be expressed as [17, 23, 24]

$$\begin{aligned} F(V,T) &= E(V) + F_{\mathrm{vib}}(\omega(V),T) \\ &= E(V) + k_{\mathrm{B}}T \sum_{\mathbf{q}} \sum_{j} \ln\left\{2\sinh\left(\frac{\hbar\omega_{\mathbf{q},j}(V)}{2k_{\mathrm{B}}T}\right)\right\} \\ &\equiv E(V) + \tfrac{1}{2}\sum_{\mathbf{q}} \sum_{j} \hbar\omega_{\mathbf{q},j}(V) + k_{\mathrm{B}}T \sum_{\mathbf{q}} \sum_{j} \ln(1 - \mathrm{e}^{-\hbar\omega_{\mathbf{q},j}(V)/k_{\mathrm{B}}T}), \end{aligned} \tag{1}$$

where E is the static contribution to the internal energy. The second and third terms on the right-hand side of equation (1) are contributions to the free energy from zero-point motion and thermal excitation, respectively. At zero pressure, the Gibbs free energy equals the Helmholtz free energy and the equilibrium crystal structure at a given temperature T can be found by minimizing the Helmholtz free energy with respect to the structure parameters such as the lattice constants in our case.

The equation of state is readily obtained from the free energy by the following expression:

$$p(V,T) = -\left(\frac{\partial F}{\partial V}\right)_T = -\left(\frac{\mathrm{d}E}{\mathrm{d}V}\right) - \left(\frac{\partial F_{\mathrm{vib}}}{\partial V}\right)_T$$
$$= -\left(\frac{\mathrm{d}E}{\mathrm{d}V}\right) + \frac{1}{V}\sum_{\mathbf{q},j}\gamma_j(\mathbf{q},V)\varepsilon(\omega_j(\mathbf{q})), \tag{2}$$

where $\gamma_j(\mathbf{q}, V)$ is the Grüneisen constant for the $(\mathbf{q}, j)$ phonon mode, defined as

$$\gamma_j(\mathbf{q},V) = -\frac{\partial \ln \omega_j(\mathbf{q},V)}{\partial \ln V} = -\frac{\partial \omega_j(\mathbf{q},V)}{\partial V}\frac{V}{\omega_j(\mathbf{q},V)}, \tag{3}$$

and $\varepsilon(\omega_j(\mathbf{q}))$ is the vibrational contribution to the internal energy from the $(\mathbf{q}, j)$ phonon mode, defined by

$$\varepsilon_j(\mathbf{q},V,T) = \hbar\omega_j(\mathbf{q},V)\left[\frac{1}{2} + \frac{1}{\exp(\hbar\omega_j(\mathbf{q},V)/k_{\mathrm{B}}T) - 1}\right]. \tag{4}$$

The vibrational entropy S is described by

$$S(V,T) = -\left(\frac{\partial F}{\partial T}\right)_V = k_{\mathrm{B}}\sum_{\mathbf{q},j}\left\{-\ln[1 - \mathrm{e}^{-\hbar\omega_{\mathbf{q},j}(V)/k_{\mathrm{B}}T}] + \frac{\hbar\omega_{\mathbf{q},j}(V)/k_{\mathrm{B}}T}{\exp(\hbar\omega_{\mathbf{q},j}(V)/k_{\mathrm{B}}T) - 1}\right\}. \tag{5}$$

The heat capacity per unit cell at constant volume can be obtained from

$$C_V(V,T) = -T\left(\frac{\partial^2 F_{\mathrm{vib}}}{\partial T^2}\right)_V = k_{\mathrm{B}}\sum_{\mathbf{q},j}\left(\frac{\hbar\omega_{\mathbf{q},j}(V)}{2k_{\mathrm{B}}T}\right)^2 \frac{1}{\sinh^2(\frac{\hbar\omega_{\mathbf{q},j}(V)}{2k_{\mathrm{B}}T})}. \tag{6}$$

The linear thermal expansion coefficients of the cell dimensions of a lattice can be written as

$$\alpha_i = \frac{1}{a_i}\frac{\partial a_i}{\partial T}. \tag{7}$$

An alternative expression can be found using Grüneisen formalism [18]. For a cubic structure which depends only on one lattice parameter a, the linear thermal expansion coefficient becomes

$$\alpha = \frac{1}{a_0^2\left.\frac{\partial^2 E}{\partial a^2}\right|_0}\sum_{\mathbf{q},j} c_v(\mathbf{q},j)\frac{-a_0}{\omega_{0\mathbf{q},j}}\left.\frac{\partial\omega_{\mathbf{q},j}(V)}{\partial a}\right|_0, \tag{8}$$

where $c_v(\mathbf{q}, j)$ is the contribution of the phonon mode $\mathbf{q}, j$ to the specific heat, $a_0^2(\partial^2 E/\partial a^2)|_0 = 9B_0V_0$ for the $B1$ phase of the alkali hydrides, B_0 is the bulk modulus, and V_0 is the equilibrium volume of the primitive unit cell at static equilibrium lattice parameter.

2.2. Computational details

The electronic structures, structural properties, phonon dispersions and thermodynamic properties were calculated using the plane wave pseudopotential code ESPRESSO [19]. The core–valence electron interaction is described by Vanderbilt pseudopotentials [20] with Perdew–Zunger (PZ) [21] LDA and Perdew–Burke–Ernzerhof (PBE) [22] GGA for the exchange–correlation functionals. As it has been demonstrated that the Compton profiles calculated by the pseudopotential method excluding the core electrons are in rather poor agreement with experiment [16], we explicitly include the semi-core electrons in the valence states. The valence electronic configurations are $1s^2 2s^1$ and $2s^2 2p^6 3s^1$ for Li and Na respectively. The electronic wavefunctions and charge densities were expanded in plane-wave basis sets. We used an 80 Ryd cut-off for wavefunctions and 960 and 640 Ryd charge density

cut-offs for LiH and NaH respectively. The Brillouin-zone integrations have been performed using a $8 \times 8 \times 8$ special k-point set. Phonon frequencies and phonon densities of state were calculated on a $4 \times 4 \times 4$ special k-point mesh (this includes the high symmetry points shown in the phonon dispersion curves). Dynamical matrices on this grid have been calculated and the real-space interatomic force constants were obtained by inverse Fourier transformation. The complete phonon dispersion curves were then obtained by interpolating the dynamical matrices using these force constants. The zero-point motion and temperature effect on the properties of the systems are taken into account by minimizing the Helmholtz free energies as a function of structural parameters [23, 24] at constant temperature and zero pressure. We used a very large k-point grid, $20 \times 20 \times 20$, for BZ sampling in calculating the free energies and related thermodynamic properties.

3. Results and discussion

3.1. Structural properties

The structural properties of LiH and NaH in the $B1$ phase have been determined by fitting the calculated Helmholtz free energies as a function of volume at a certain temperature to either the Murnaghan equation of state [25]

$$F(V) = F(V_0) + \frac{B_0 V}{B_0'}\left[\frac{(V_0/V)^{B_0'}}{B_0' - 1} + 1\right] - \frac{B_0 V_0}{B_0' - 1}, \tag{9}$$

or the Birch third-order equation of state [26]

$$F(V) = F(V_0) + \tfrac{9}{8} B_0 V_0 [(V_0/V)^{2/3} - 1]^2 + \tfrac{9}{16} B_0 V (B_0' - 4)[(V_0/V)^{2/3} - 1]^3 + \mathrm{O}[(V_0/V)^{2/3} - 1]^4 \tag{10}$$

where B_0 and B_0' denote the bulk modulus and its pressure derivative at equilibrium volume V_0. The Murnaghan equation of state is used for the $B1$ phase and the $B2$ phase is better fitted to the Birch third-order equation of state. The LDA results are compared with GGA and available first principles density functional calculation results and experimental values.

We present in table 1 the equilibrium lattice constant a_0, bulk modulus B_0, and pressure derivative of the bulk modulus B_0' for LiH and LiD in the $B1$ phase calculated using different approximations for exchange–correlation functionals. It is evident that the explicit inclusion of the lattice motion energy greatly improves the agreement between theory and experiments. The PBE lattice constant with the zero-point energy included is closest to the experiments [1, 2, 7]. For LiH at 300 K, LDA gives $a_0 = 7.58$ au which is 1.8% smaller than experiment and GGA gives $a_0 = 7.78$ au which is 0.8% larger. While the LDA bulk modulus is in good agreement with the experimental values, the PBE underestimates the bulk modulus. The lattice parameters calculated by others using density functional theory vary greatly. Ours are closest to the full potential calculation of Lebègue *et al* [11], who used the zero-point energies calculated by Roma *et al* in their calculations.

The corresponding structural properties of NaH in the $B1$ phase calculated using both approximations for the exchange–correlation functional are given in table 2. As in the case of lithium hydrides, the lattice constant from the PBE calculation including the zero-point motion is in excellent agreement with the experiment [9]. At 300 K, the LDA gives $a_0 = 9.07$ au, which is 2.3% smaller than experiment, and the GGA gives $a_0 = 9.35$ au, which is 0.8% larger. The LDA and PBE bulk moduli at 300 K are close to the upper and lower limits of the experimental results and the average value of 196 GPa is in good agreement with the experimental value of 194 GPa. Our PBE lattice constants are in good agreement with the values given by

Table 1. Equilibrium lattice constant a_0 (bohr), bulk modulus B_0 (kbar), and pressure derivative of the bulk modulus B_0' as a function of temperature (K) for LiH and LiD in the $B1$ phase using different approximations for exchange–correlation functionals. GGA results from other calculations are shown in the brackets.

	a_0	B_0	B_0'	T
LDA (PZ) (this work)	7.389	408	3.64	0
	7.544, 7.512	358, 367	3.51, 3.54	0[a]
	7.576, 7.549	332, 339	3.76, 3.81	300[a]
GGA (PBE) (this work)	7.574	365	3.63	0
	7.736, 7.704	316, 325	3.59, 3.62	0[a]
	7.782, 7.753	281, 288	4.18, 4.24	300[a]
Experiments	7.716, 7.690[c]			298
	7.717, 7.688[d]	336, 340[d]		298
	7.718, 7.691[e]	322[e]	3.53[e]	298
		317 ± 4[j]	3.4 ± 0.1[j]	294
Calculations	7.39(7.58)[f]	400(361)[f]		0
	7.54(7.71)[f]	359(339)[f]		0[a]
	7.33[g]	390[g]		0
	7.48, 7.45[g]	350, 360[g]		0[a]
	7.442(7.606)[h]	405(362)[h]		0
	7.631(7.827)[h]	333(288)[h]		298[a]
	7.421[i]			0
	7.559[i]	366[i]	3.40[i]	0[a]
	7.574[i]			298[a]

[a] Zero-point energy included.
[b] The second value of the same quantity is for LiD.
[c] Reference [7].
[d] Reference [1].
[e] Reference [2].
[f] Reference [11].
[g] Reference [10].
[h] Reference [27].
[i] Reference [4].
[j] Reference [5].

Ke *et al* [28]. The seemingly better agreement of the LDA values with the experimental results reported in [6] is in fact due to a poor sampling of the BZ as pointed out in [11].

It should be noted that, when using the pseudopotentials with only the outermost 1s electron as the valence electron for Li and Na, the calculated lattice constants are in very poor agreement with experiments even when linear core correction is included, with the only exception of lithium hydrides using the Von Barth and Car type exchange–correlation functional within the LDA approximation [10].

3.2. Phonon dispersions

The phonon dispersions for both $B1$ and $B2$ phases of the alkali hydrides were also calculated. The phonon dispersion curve of LiD at 300 K for the $B1$ phase is shown in figure 1(a) and compared with the experimental values (solid symbols). The overall agreement is very good, which justifies the validity of our pseudopotentials. Also shown in figure 1 are the phonon dispersion curves for LiH and NaH in the $B1$ phase (figures 1(b) and (c) respectively). The three sets of phonon dispersion curves are quite similar, which comes from the similar electronic

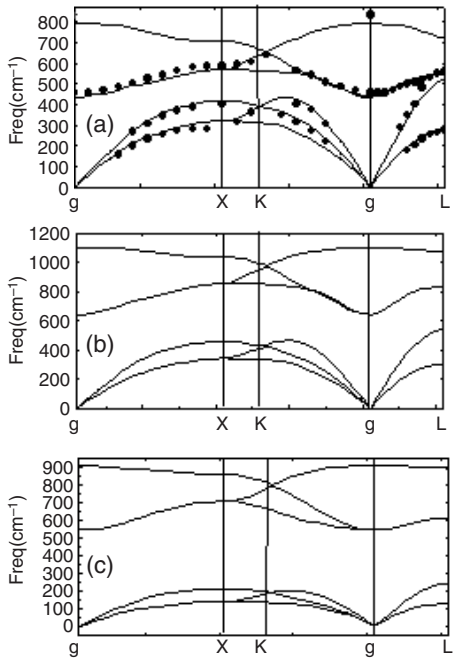

Figure 1. Phonon dispersion curves along major symmetry directions of the BZ for the $B1$ phase of (a) LiD at 300 K (zero-point motion effect included), $a_0 = 7.55$ au, (b) LiH at 0 K and (c) NaH at 0 K. Experimental data [35] at 0.1 MPa are shown in (a) as filled symbols. All calculations were performed at zero pressure.

Table 2. Equilibrium lattice constant a_0 (bohr), bulk modulus B_0 (kbar), and pressure derivative of the bulk modulus B_0' as a function of temperature (K) for NaH in the $B1$ phase using different approximations for exchange–correlation functionals. GGA results from other calculations are shown in the brackets.

	a_0	B_0	B_0'	Temp.
LDA (PZ) (this work)	8.86	272	3.80	0
	9.00	241	3.65	0[a]
	9.07	208	3.75	300[a]
GGA (PBE) (this work)	9.14	229	3.62	0
	9.27	209	3.53	0[a]
	9.35	184	3.50	300[a]
Experiment	9.28[b]	194 ± 20[b]	4.4 ± 0.5[b]	298
Theory	9.02[c]	270[c]	3.7[c]	0
	9.30[c]	200[c]	4.1[c]	0[a]
	9.108[d]			0
	9.235[d]	234[d]		0[a]
	9.362[d]	210[d]		300[a]
	8.955(9.201)[e]	272(240)[e]		0
	9.175(9.403)[e]	226(202)[e]		298[a]

[a] Zero-point energy included.
[b] Reference [9].
[c] Reference [6].
[d] PW-GGA results from reference [28].
[e] Reference [27].

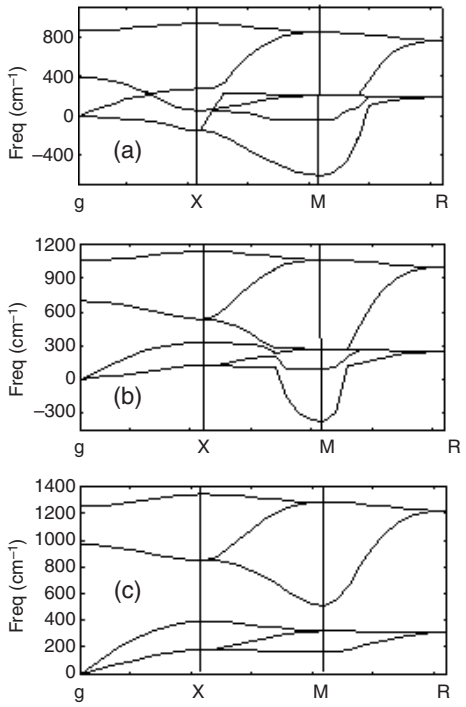

Figure 2. Phonon dispersion curves for NaH in the $B2$ phase at 0 K. (a) 0 GPa, (b) 10.97 GPa and (c) 29.5 GPa.

structure of the outermost shell for all alkali metals. Due to the different atomic masses, there is no phonon bandgap between the acoustic and optical phonon branches for LiD and the largest phonon bandgap is found in NaH.

We show in figure 2 the phonon dispersion curves for NaH $B2$ structure at pressures of 0, 10.97 and 29.5 GPa. At zero pressure (figure 2(a)), one of the transverse acoustic branches is unstable around the M point as it is in the case of LiH. But with increasing pressure, the M point phonon becomes stable around 17 GPa. Figure 2(c) shows the dispersion curves at 29.5 GPa (close to our calculated $B1$-to-$B2$ transition pressure of 29.6 GPa). We can see that the $B2$ structure of NaH is stable at the $B1$-to-$B2$ transition pressure and beyond.

For the $B2$ structure of LiH, if no Fermi surface smearing parameter is used in the calculation, the instability of the transverse acoustic branch will persist. This is caused by the very small bandgap and the band-closing phenomenon with applied pressure. In our calculation, we used a smearing parameter of 0.05 Ryd and the unstable branch becomes stable at pressure higher than 160 GPa.

3.3. Thermodynamic properties

Using the phonon frequencies interpolated from the phonon dispersions, we calculated the thermodynamic properties of lithium deuteride, lithium hydride and sodium hydride. Because of the large zero-point motion and thermal expansion in our studied systems, the phonon frequencies are usually computed at more than 15 lattice parameters with an average increment of 0.05 bohr around the static equilibrium geometry and the results interpolated by cubic polynomials using the Akima method [29] to get their dependence on lattice constant. For

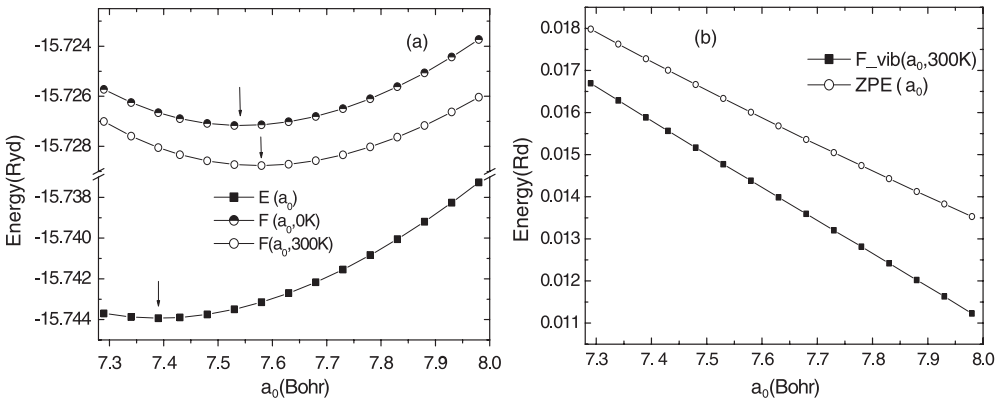

Figure 3. (a) Static energy, 0 and 300 K free energy as a function of lattice constant a_0 (arrows denote the minima of the corresponding curves) and (b) zero-point energy (ZPE) and 300 K vibrational free energy as a function of lattice constant a_0 for LiH in $B1$ phase.

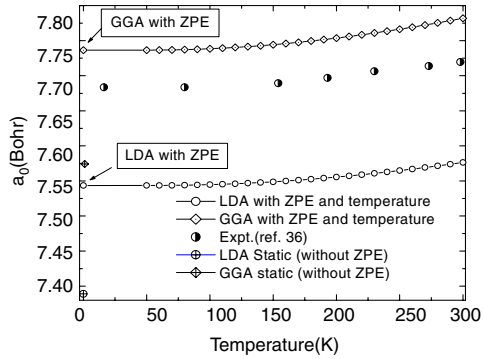

Figure 4. The equilibrium lattice constant a_0 from both LDA and GGA calculations as a function of temperature for LiH in the $B1$ phase.

LiH and LiD LDA calculations, the lattice parameters range from 7.29 to 7.98 au; while for GGA calculations, the corresponding range is 7.47–8.17 au. For NaH GGA calculations, the chosen lattice parameter range is from 9.04 to 9.50 au as compared to 7.61–9.46 au for LDA calculations. Such a wide range of lattice constant for the LDA case is essential for calculating both the thermodynamic properties at zero pressure and the equation of state at 300 K. The volume dependence of the free energy is then calculated using equation (1) and fitted to the Murnaghan equation of state (we have found in our case that the Birch–Murnaghan equation of state is not suitable for the $B1$ phase). This gives us, at any temperature T, the equilibrium lattice parameter, bulk modulus B_0, and its pressure derivative B_0'. The lattice constant dependence of the various energy terms at different temperatures can be found in figure 3.

The variations of the lattice constant with temperature for LiH in the $B1$ phase calculated with both LDA and GGA approximations are shown in figure 4 along with experimental values. It can be seen that the zero-point motion greatly affects the equilibrium lattice constants and the calculated LDA and GGA results bracket the experimental values. The coefficients of linear thermal expansion at any temperature are obtained using both the Grüneisen formalism and direct numerical differentiation of the lattice parameters. The results are shown in figures 5

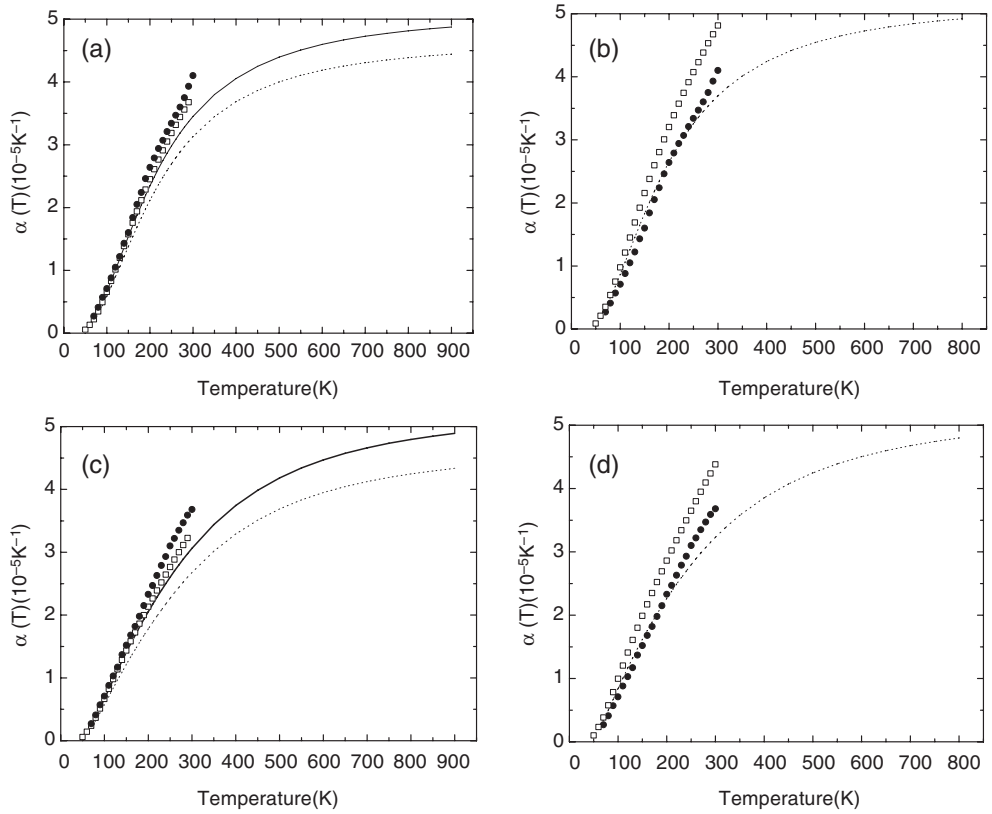

Figure 5. Coefficients of linear thermal expansion for LiD ((a) LDA, (b) GGA) and LiH ((c) LDA, (d) GGA) as a function of temperature calculated with LDA-PZ and GGA-PBE approximations. Dotted and solid lines are calculated using the Grüneisen formalism [18] at the static and zero-point motion corrected equilibrium geometries respectively. Open squares represent the direct numerical differentiation of the lattice constants. Filled circles are the experimental data [32].

and 6. For LiD and LiH, the agreement between experiment and the LDA direct numerical differentiation of the lattice parameters remains excellent at temperatures below 300 K. We can also see that if the static equilibrium parameters are used in equation (8) the agreement between the two curves (shown by the dotted line and open squares) calculated by the two methods is poor even at very low temperature. This is mainly caused by the large zero-point correction of the lattice parameter and bulk modulus. The agreement becomes much better when the zero-point corrected equilibrium lattice parameters and bulk moduli are substituted for the static ones as shown in the figures by the solid lines in the case of LDA. The GGA results tend to overestimate the experimental values in this case, but the agreement is still very good below 250 K if the Grüneisen formalism is adopted.

The constant volume heat capacities at zero pressure were calculated using equation (6), in which we use the interpolated phonon frequencies computed at the lattice constant that minimizes the respective free energy at each temperature T. The constant pressure heat capacity is linked to the constant volume heat capacity by $C_P(T) = C_V(T) + TB_0(T)V_0(T)\alpha_V^2(T)$, where V_0 is the volume of the primitive unit cell, α_V the volumetric thermal expansion coefficient (which is three times the linear thermal expansion coefficient in our case) and B_0 the bulk modulus. All the quantities are evaluated at each of the temperatures

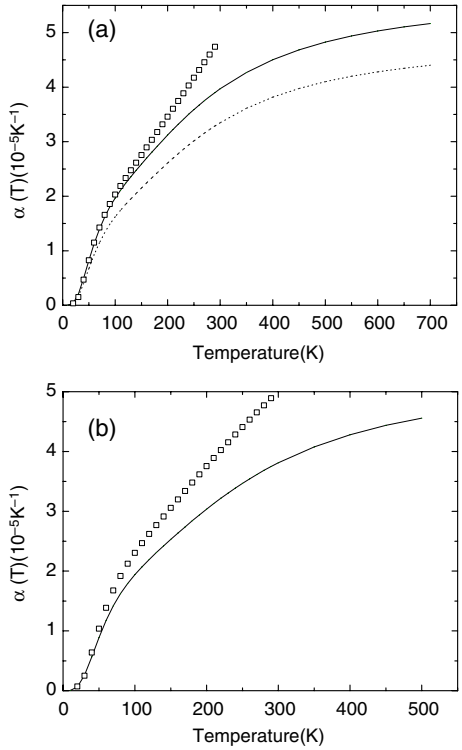

Figure 6. Coefficients of linear thermal expansion for NaH as a function of temperature calculated with (a) LDA-PZ and (b) GGA-PBE approximations. Dotted and solid lines are calculated using the Grüneisen formalism [18] at the static and zero-point motion corrected equilibrium geometries respectively. Open squares represent the direct numerical differentiation of the lattice constants.

considered. We present results on the heat capacities in figures 7 and 8 ((a) and (b)). We can see that the agreement with experiments is excellent except in the high temperature range of LiH GGA calculation.

Finally, similar to the heat capacity, the vibrational entropies for NaH were calculated using equation (5) and displayed in figure 8 ((c) and (d)). It is seen that, even at high temperature, the agreement with the experimental data is still excellent for LDA calculation while GGA slightly overestimates the experimental values.

3.4. Equation of states and $B1$-to-$B2$ phase transition

The structural phase transition of NaH, KH and CsH from the low-pressure rock-salt ($B1$) structure to the high-pressure caesium chloride ($B2$) structure has been observed at pressures lower than 30 GPa [9, 30]. We have calculated the equation of states and the $B1$-to-$B2$ transition pressures for LiH and NaH systems. The EOS is calculated both at zero temperature and 300 K. The $B1$-to-$B2$ phase transition in LiH has not been observed up to now. There have been many theoretical predictions for this phase transition and the estimated transition pressure ranging from about 300 to 600 GPa. Given the large discrepancies of the theoretical predictions, we only calculated in this paper the transition pressure at zero temperature, neglecting the vibrational effect. For NaH, the transition pressure is also computed at 300 K. All the calculations are done with the LDA approximation only for electronic exchange and correlation.

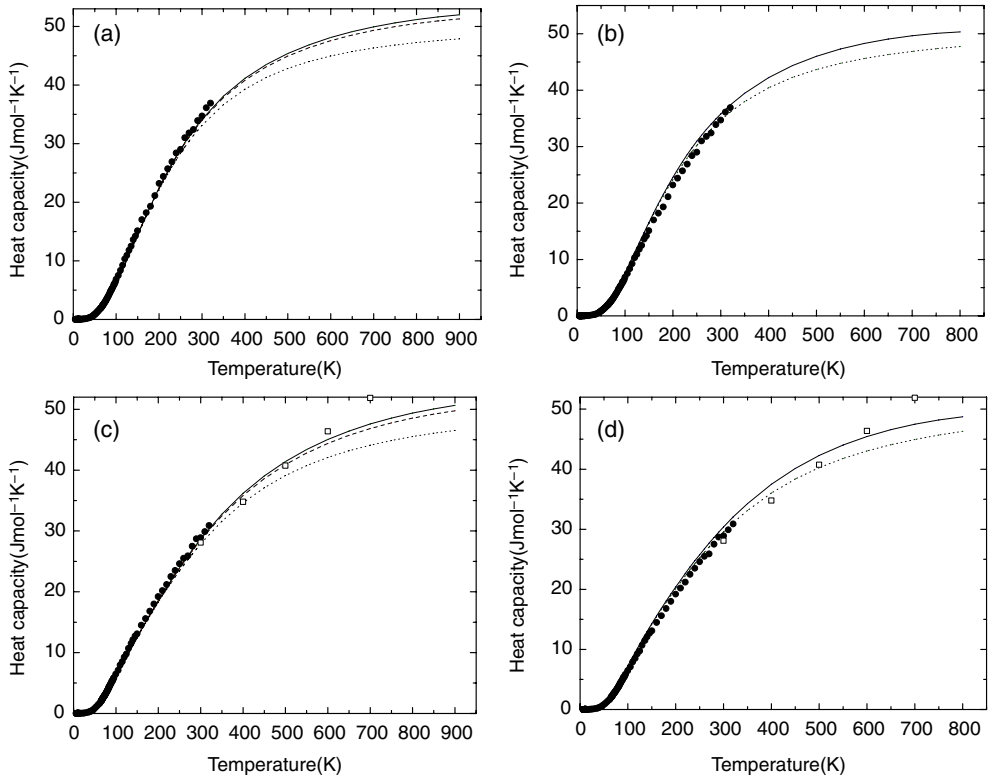

Figure 7. Heat capacities for LiD ((a) LDA, (b) GGA) and LiH ((c) LDA, (d) GGA) as a function of temperature calculated with LDA-PZ and GGA-PBE approximations. The dotted line denotes the constant volume heat capacity. Dashed and solid lines are the constant pressure heat capacities obtained using the two types of linear thermal expansion coefficients calculated by the Grüneisen formalism at the static and zero-point motion corrected equilibrium geometries respectively. Filled circles are the experimental data [33]. Open squares are high temperature experimental values from [34].

For the $B1$ phase, we use the Vinet form [31] (universal equation of state) to fit the calculated free energies because the Murnaghan equation of state is too 'hard' at high pressure. As the $B2$ phase is unstable at low pressure, this fitting method will not be accurate because the free energies could only be calculated at smaller volumes far from the zero-pressure geometry. Therefore, we use equation (2) to calculate the volume dependence of the pressure directly. We present in figure 9 the 300 K pressure-versus-volume equation of state for NaH in both $B1$ and $B2$ phases. The agreement between experiment and theory is very good.

Experimentally [9], the $B1$-to-$B2$ transition for NaH is reversible and happens at a transition pressure of 29.3 ± 0.9 GPa and a volume fraction $V/V_0 = 0.61 \pm 0.01$. Our LDA calculation at zero temperature, as shown in figure 10(a), gives a transition pressure of 31.8 GPa at a volume fraction $V/V_0 = 0.63$. The transition pressure is determined from the common tangent of the static energy–volume curves for $B1$ and $B2$ phases. The change in volume at the transition pressure is 11.3% of the $B1$ phase volume. The calculated transition pressure is in better agreement with the experiment than the theoretical result of 37 GPa from [3].

In order to account for the vibrational effect on the phase transition pressure, we calculated the free energies for the $B1$ and $B2$ phases at different volumes by the same method as used

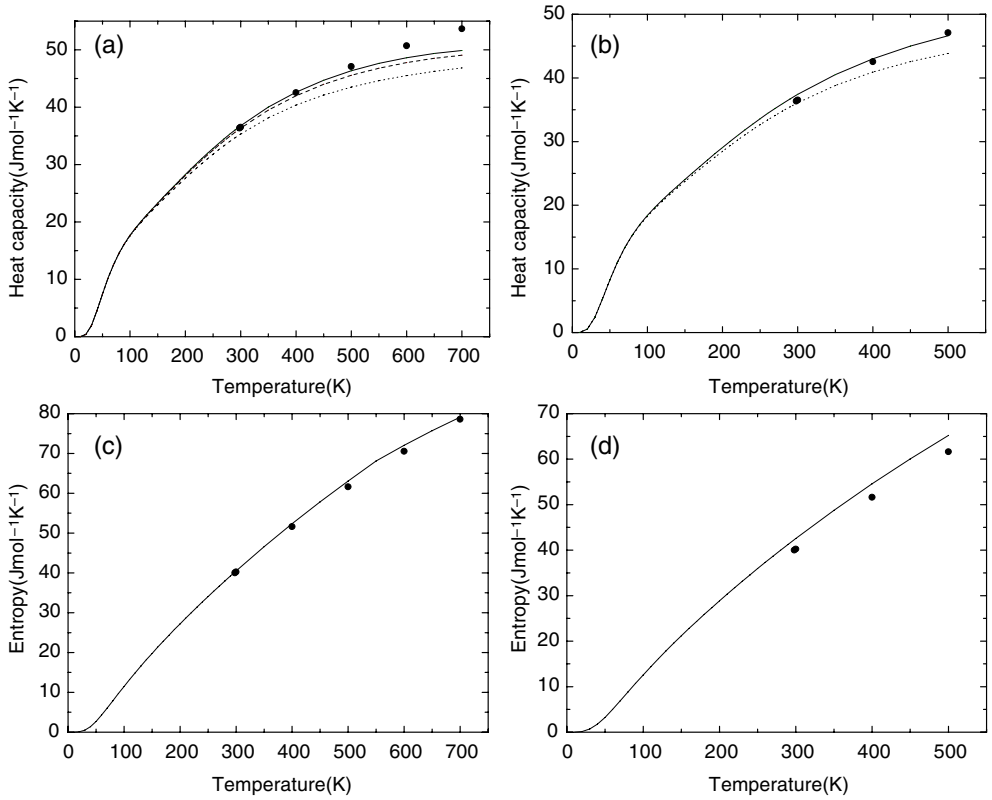

Figure 8. Heat capacities ((a) LDA, (b) GGA) and vibrational entropies ((c) LDA, (d) GGA) for NaH as a function of temperature calculated with LDA-PZ and GGA-PBE approximations. Dotted lines denote the constant volume heat capacity. Dashed and solid lines ((a) and (b)) are the constant pressure heat capacities obtained using the two types of linear thermal expansion coefficients calculated by the Grüneisen formalism at the static and zero-point motion corrected equilibrium geometries respectively. Filled circles are the experimental data [34]. Solid lines in (c) and (d) are the results of this work.

to calculate the thermodynamic properties. From the 300 K Helmholtz free energy–volume curves (shown in figure 10(b)), we determined the transition pressure of 29.6 GPa at a volume fraction $V/V_0 = 0.60$. This is in excellent agreement with the experiment. The change in volume at the transition pressure is 7% of the $B1$ phase volume at the same pressure, which is smaller than the experimental value of 10% at 29.3 GPa. Due to the rather scattered nature of the experimental points around the transition pressure, the uncertainty for the volume change may be large.

The pressure-versus-volume equation of state at 300 K for LiD and LiH at $B1$ phase is shown in figure 11. All the curves are fitted by the Vinet equation of state either using the experimental or calculated bulk modulus and its pressure derivative. The two curves for LiD and LiH are very close to each other and to the zero-temperature (zero-point motion included) curve fitted using the data given by Hamma *et al*. The overall agreement with experiment is good up to about 130 GPa. The seemingly better agreement between the experimental and zero-temperature theoretical data by Martins [6] (the zero-point motion effect included) is in fact due to a poor sampling in the evaluation of the zero-point energy which makes the calculated zero-pressure lattice parameter (7.63 bohr) much larger than the results by other

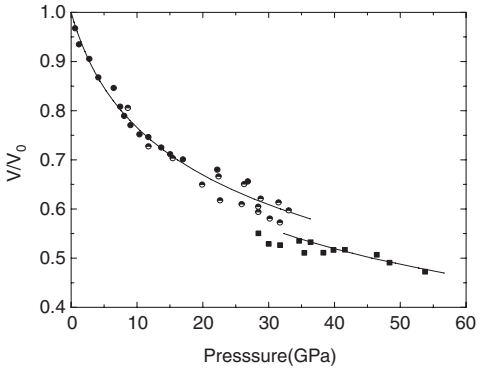

Figure 9. Equation of state for NaH $B1$ and $B2$ phases calculated with the LDA-PZ approximation. The upper solid line is for the $B1$ phase fitted to the Vinet [31] equation of state. The lower solid line is for the $B2$ phase calculated using equation (2). The filled circles and squares are the experimental values for $B1$ and $B2$ phases respectively [9]. The half-filled circles are from the experimental work of Hochheimer *et al* ($B1$) [30].

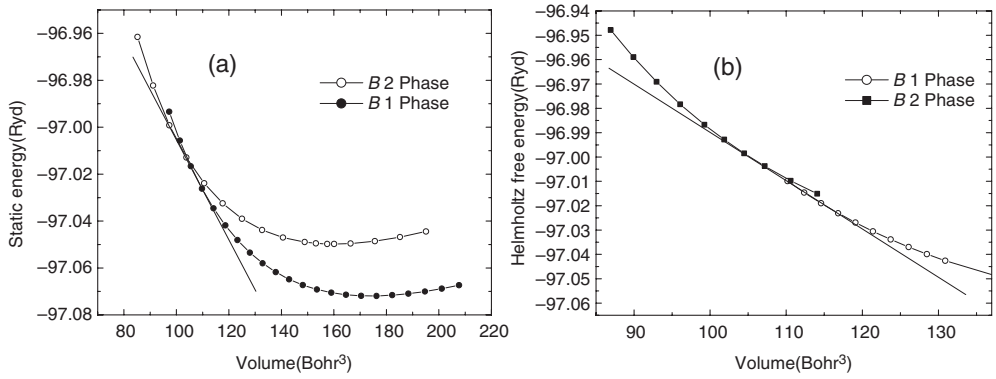

Figure 10. Energy versus volume relationship calculated with the LDA-PZ approximation for NaH $B1$ and $B2$ phases at (a) 0 K and (b) 300 K. The solid line denotes the common tangent of the two curves along which the phase transition happens.

authors. In drawing the p–V curves of our calculations, we used the theoretical equilibrium volume instead of the experimental one. If the experimental equilibrium volume is used, the agreement with experiment will be even better. Using similar procedure as we did for NaH, we found for LiH the $B1$-to-$B2$ transition pressure at zero temperature to be 308 GPa at a volume fraction $V/V_0 = 0.329$ or $V/V_0 = 0.289$ if V_0 is taken as the average experimental equilibrium volume ($a_0 = 7.717$ au). Our transition pressure is very close to the value of 313 GPa found by Wang *et al* [15] and also in good agreement with the calculation of Lebegue *et al* [11]. Their calculated transition pressure is 329 GPa at a volume fraction of $V/V_0 = 0.29$, where V_0 is the experimental equilibrium volume.

4. Conclusions

In conclusion, using plane wave pseudopotential density functional theory and density functional perturbation theory within the framework of the quasiharmonic approximation we have calculated the phonon dispersions and thermodynamic properties for the lighter alkali

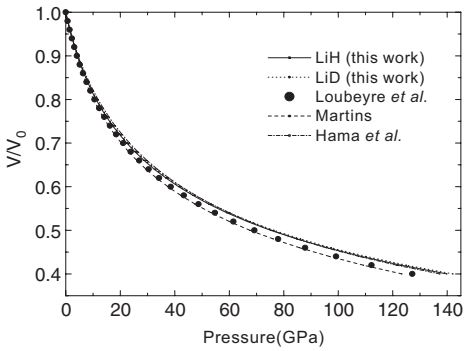

Figure 11. Equation of states for LiD and LiH $B1$ phases calculated with the LDA-PZ approximation. The filled circles are the fitted values by the Vinet equation of state using the experimental bulk modulus and its pressure derivative from Loubeyre *et al* [2]. Temperature and zero-point effects are not taken into account.

hydrides LiD, LiH and NaH. The equation of states and $B1$-to-$B2$ phase transition are also discussed. We found it is essential to include explicitly the semi-core states in the valence states in order to make accurate calculations comparable to experiments. The calculated equilibrium lattice parameters and bulk moduli are in good agreement with experiments if the lattice vibrational effect is taken into account. From the phonon dispersion calculation, we found that the $B2$ phase is unstable at low pressure and becomes stable with increasing pressure. The calculated thermodynamic properties agree quite well with the experimental data, especially at low temperature. When the temperature dependence of the free energy is taken into account, the calculated $B1$-to-$B2$ transition pressure for NaH (29.6 GPa) is in excellent agreement with the experimental value of 29.3 ± 0.9 GPa. The transition pressure for LiH (308 GPa) is also very close to the values most recently calculated by other authors using full-potential DFT method. It is also true that in the case of large zero-point movement effect the QHA works well.

Acknowledgments

WY would like to thank Professor John Tse and Nicola Marzari for stimulating discussions and Guido Roma for providing his version of the norm-conserving pseudo-potential for Li (for comparison with our USPP calculation; the results are not included in this paper). AK would like to thank Dr Bernd Meyer for his invaluable guidance in building ultra-soft pseudopotentials. This work was supported by NSF and MOST of China through the research projects 2005CB724402, 50321101 and 50332020.

References

[1] Stephens D R and Lilley E M 1968 *J. Appl. Phys.* **39** 177
[2] Loubeyre P, Le Toullec R, Hanfland M, Ulivi L, Datchi F and Hausermann D 1998 *Phys. Rev.* B **57** 10430
[3] Ahuja R, Eriksson O and Johansson B 1999 *Physica* B **265** 87–91
[4] Hama J, Suito K and Kawakami N 1989 *Phys. Rev.* B **39** 3351
[5] Besson J M, Weill G, Hamel G, Nelmes R J, Loveday J S and Hull S 1992 *Phys. Rev.* B **45** 2613
[6] Martins J L 1990 *Phys. Rev.* B **41** 7883
[7] Anderson J L, Nasise J, Philipson K and Pretzel F E 1970 *J. Phys. Chem. Solids* **31** 613
[8] Kondo Y and Asaumi K 1988 *J. Phys. Soc. Japan* **57** 367
[9] Duclos S J, Vohra Y K, Ruoff A L, Fillipek S and Baranowski B 1987 *Phys. Rev.* B **36** 7664

[10] Roma G, Bertoni C M and Baroni S 1996 *Solid State Commun.* **98** 203
[11] Lebègue S, Alouani M, Arnaud B and Pickett W E 2003 *Europhys. Lett.* **64** 562
[12] Bellaiche L, Besson J M, Kunc K and Lévy B 1998 *Phys. Rev. Lett.* **80** 5576
[13] Barrera G D, Colognesi D, Mitchell P C H and Ramirez-Cuesta A J 2005 *Chem. Phys.* **317** 119
[14] Hybertsen M S and Louie S G 1986 *Phys. Rev.* B **34** 5390
[15] Wang Y, Ahuja R and Johansson B 2003 *Phys. Status Solidi* b **235** 470
[16] Bellaiche L and Kunc K 1997 *Phys. Rev.* B **55** 5006
[17] Born M and Huang K 1954 *Dynamical Theory of Crystal Lattices* (Oxford: Clarendon Press/Geoffrey Cumberlege)
[18] Barron T H K, Collins J G and White G K 1980 *Adv. Phys.* **29** 609
[19] Baroni S *et al* http://www.quantum-espresso.org
[20] Vanderbilt D 1990 *Phys. Rev.* B **41** R7892
[21] Perdew J P and Zunger A 1981 *Phys. Rev.* B **23** 5048
[22] Perdew P, Burke K and Ernzerhof M 1996 *Phys. Rev. Lett.* **77** 3865
[23] Xie J, de Gironcoli S, Baroni S and Scheffler M 1999 *Phys. Rev.* B **59** 965
[24] Mounet N and Marzari N 2005 *Phys. Rev.* B **71** 205214
[25] Murnaghan F D 1937 *Am. J. Math.* **49** 235
[26] Birch F 1947 *Phys. Rev.* B **71** 809–24
[27] Barrera G D, Colognesi D, Mitchell P C H and Ramirez-Cuesta A J 2005 *Chem. Phys.* **317** 119
[28] Ke X and Tanaka I 2005 *Phys. Rev.* B **71** 024117
[29] Akima H 1970 *J. ACM* **17** 589–602
[30] Hochheimer H D, Strössner K, Hönle W, Baranowski B and Filipek F 1985 *Z. Phys. Chem.* **143** 139
[31] Vinet P, Rose J H, Ferrante J and Smith J R 1989 *J. Phys.: Condens. Matter* **1** 1941
[32] James B W and Kheyrandish H 1982 *J. Phys. C: Solid State Phys.* **15** 6321
[33] Yates B, Wostenholm G H and Bingham J L 1974 *J. Phys. C: Solid State Phys.* **7** 1769
[34] Chase M W Jr 1998 *NIST-JANAF Themochemical Tables,* 4th edn; *J. Phys. Chem. Ref. Data* **9** 1 (Monograph)
[35] Verble J L, Warren J L and Yarnell J L 1968 *Phys. Rev.* **168** 980
[36] Smith D K and Leider H R 1968 *J. Appl. Crystallogr.* **1** 246